Electronic Supplementary Information for

Block Copolymer Derived 3-D Interpenetrating Multifunctional Gyroidal Nanohybrid for Electrical Energy Storage

J. G. Werner[a,b], G. G. Rodríguez-Calero[b], H. D. Abruña[b] and U. Wiesner[a]*

[a.] Department of Materials Science and Engineering, Cornell University, Ithaca, NY 14853, USA. E-mail: ubw1@cornell.edu.
[b.] Department of Chemistry and Chemical Biology, Cornell University, Ithaca, NY 14853, USA.

The supplementary information includes:

Supplementary Figures S1 to S5
Supplementary Tables S1 and S2
Detailed experimental procedures

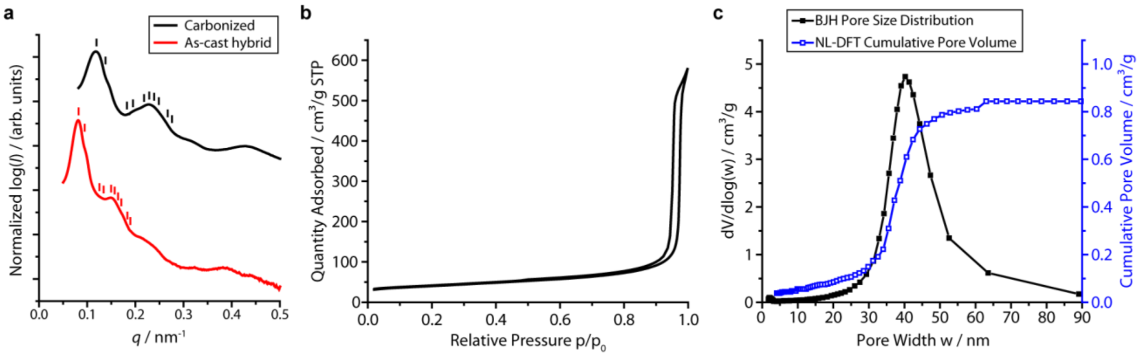

Figure S1. Gyroidal mesoporous carbon (G^{D}MC) characterization. (a) Small-angle X-ray scattering pattern of G^{D}MC as-cast hybrid (bottom, red) and after carbonization (black, top). The markings indicate expected positions for the $I\bar{a}3d$ space group lattice peaks of the double gyroid morphology with a (100) spacing of 188 nm (hybrid) and 129 nm (carbonized), respectively. (b) Nitrogen sorption isotherms of carbonized G^{D}MC. (c) BJH pore size distribution (solid symbols) and DFT cumulative pore volume (open, blue symbols) of carbonized G^{D}MC calculated from the nitrogen adsorption isotherm.

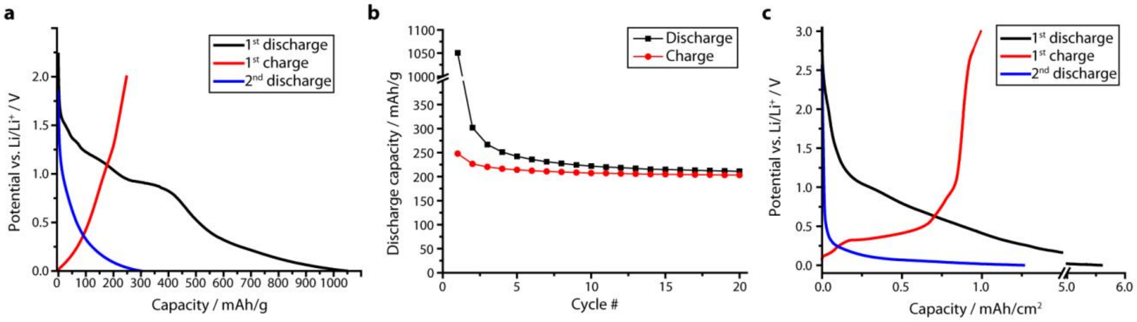

Figure S2. Galvanostatic measurements of G^DMCs. (a) Charge and discharge curves of powdered G^DMC in a standard coin cell versus lithium metal at a current of 30 mA g_C^{-1}. (b) Charge and discharge capacities of the first 22 cycles of the coin cell test demonstrating a reversible capacity of 220 mAh g^{-1}. (c) Discharge and charge curves of PPO-coated G^DMC at a current of 0.1 mA cm^{-2} (corresponding to approximately 20 mA g_C^{-1}), demonstrating reversible lithiation-delithiation through the PPO-layer.

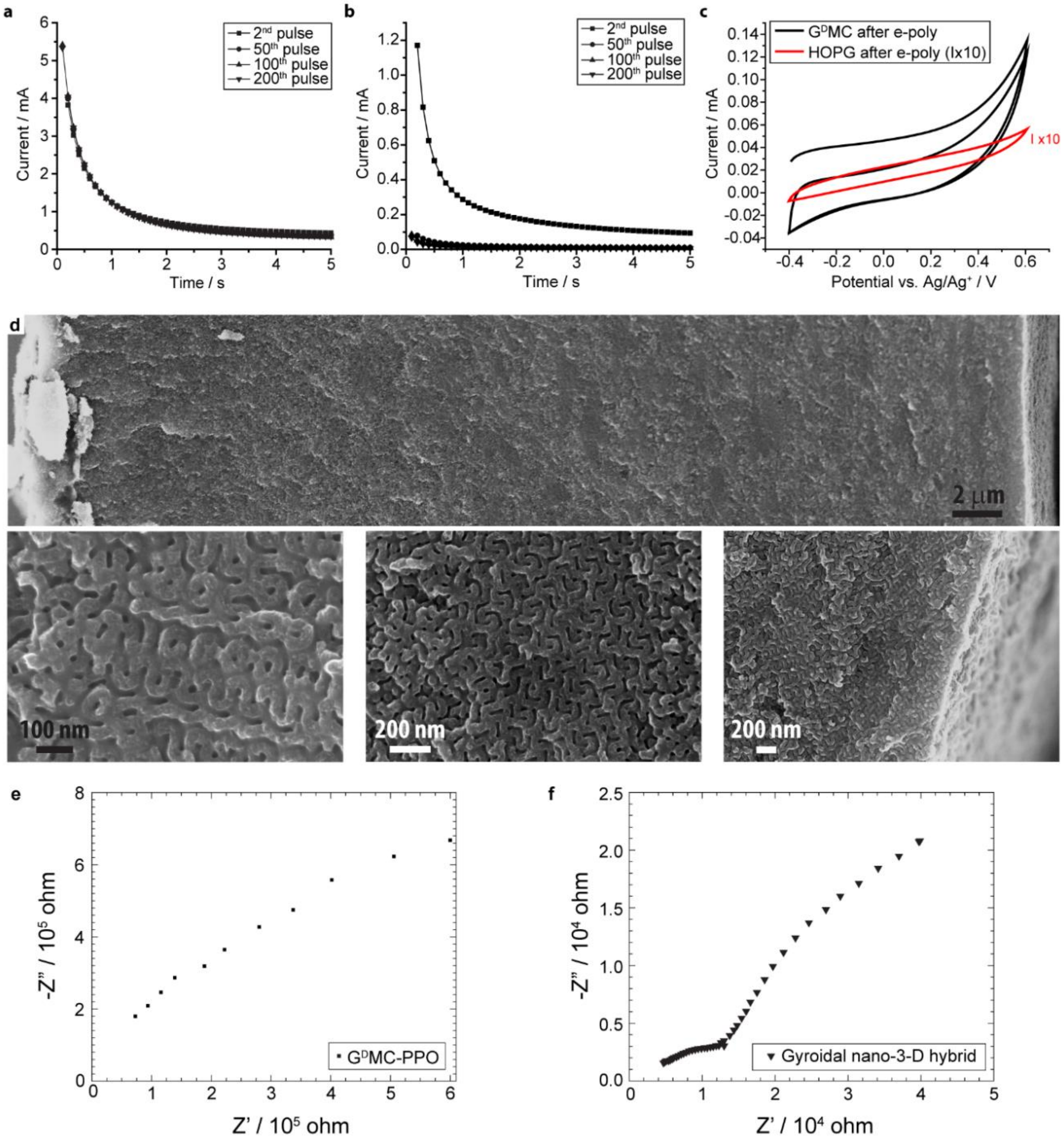

Figure S3. Electropolymerization of poly(phenylene oxide) (PPO). (a) Current-time traces of selected potentiostatic pulses at +0.6 V vs. Ag/Ag$^+$ of a G^DMC monolith in the supporting electrolyte demonstrating no change over 200 pulses. (b) Current-time traces of selected potentiostatic deposition pulses of PPO on a flat carbon substrate (highly oriented pyrolytic graphite, HOPG) at +0.6 V vs. Ag/Ag$^+$ showing the very fast decrease in current with number of pulses. (c) Cyclic voltammograms after pulsed potentiostatic PPO deposition in the same solutions of G^DMC and HOPG exhibiting no oxidation peak and much larger double layer current for G^DMC (current of the HOPG is multiplied by a factor of 10). (d) Cross-sectional SEM images of PPO-coated G^DMC at low magnification (top) and at higher magnifications (bottom) close to the left surface, the film center, and the right surface (from left to right) suggesting homogeneous PPO coating of the gyroidal mesopores throughout the monolith. (e,f) Nyquist diagrams of the electrochemical impedance spectroscopy results of (e) a PPO-coated G^DMC and (f) a 3-D gyroidal nanohybrid. Data were taken with an AC-amplitude of 5 mV on open circuit voltage in the frequency range of 20 MHz to 1 Hz.

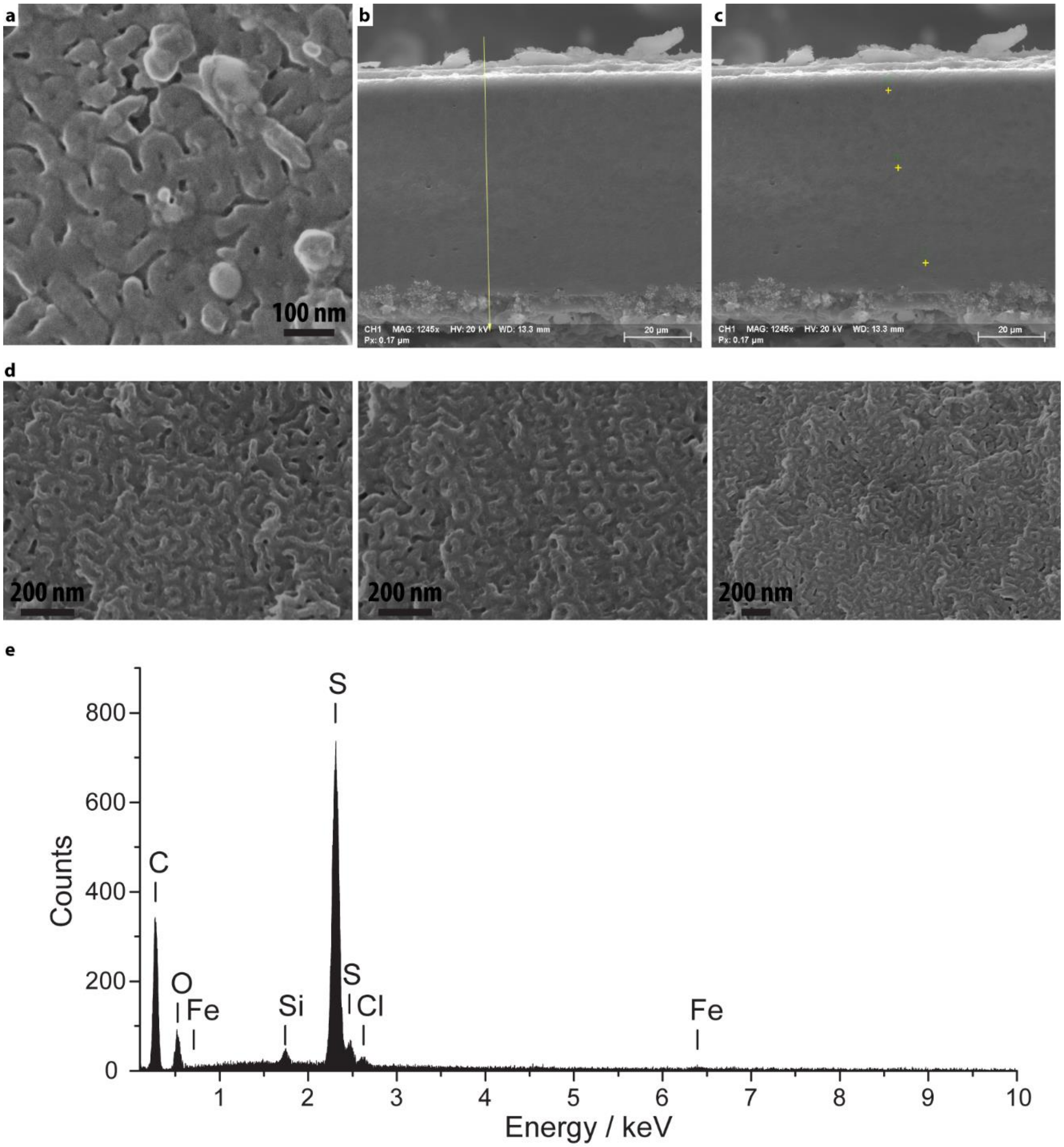

Figure S4. Cathode composite infiltration. (a) High-resolution SEM image of the PPO-coated $\mathrm{G^DMC}$ monolith surface after sulfur infiltration evidencing remaining porosity, which in turn signifies that no appreciable amount of excess external sulfur has deposited on the monolith surface during the sulfur infiltration process. (b) Cross-sectional SEM image of the fully integrated sulfur-PEDOT backfilled PPO-coated $\mathrm{G^DMC}$ described in the main text with the arrow showing the position of the line scan plotted in Fig. 3c. (c) The same cross-sectional SEM image with the marks showing the position of quantified EDS-spectra with estimated carbon to sulfur weight ratios of 3.8, 3.0, and 3.4 at the top, middle, and bottom of the monolith, respectively. (d) High-magnification SEM images of a 3-D gyroidal nanohybrid ($\mathrm{G^DMC}$ coated with PPO and back-filled with sulfur and PEDOT) at different positions across the monolith cross-section suggesting fairly homogeneous infiltration efficiency. (e) Full energy dispersive X-ray (EDX) spectrum of a 3-D gyroidal nanohybrid with expected energies of different elements indicated in the graph.

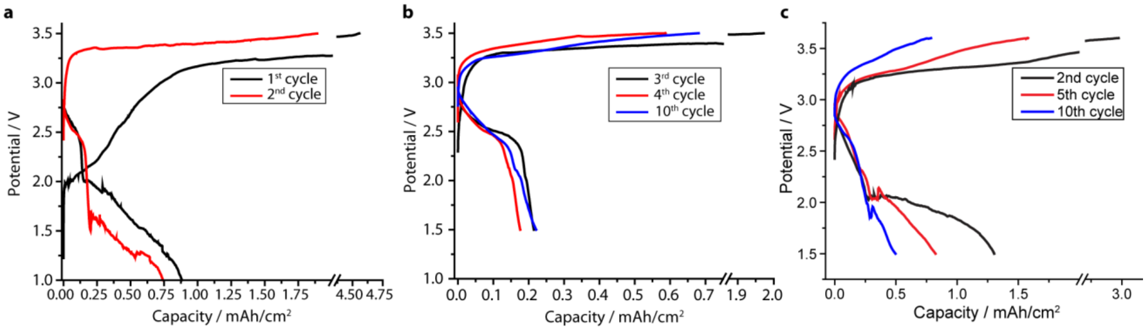

Figure S5. Electrochemical characterization of a solid-state 3-D gyroidal nanohybrid. (a) Solid-state charge-discharge curves of the first two cycles that were run over the potential window of 1-3.5 V at a current rate of 0.125 mA cm^{-2}. (b) Charge and discharge curves of selected cycles that were run in the potential window of 1.5-3.5 V at a current rate of 0.125 mA cm^{-2}. (c) Charge and discharge curves of selected cycles that were run in the potential window of 1.5-3.6 V at a current rate of 0.25 mA cm^{-2}.

Table S1.

Triblock terpolymer ISO molar mass and composition.

M_n* / kg/mol	f_w † (PI)	f_w† (PS)	f_w† (PEO)	M_w/M_n ‡
129.6	15.4%	31.4%	53.2%	1.09

* Obtained from ^{1}H-NMR and GPC analysis. † Obtained from ^{1}H-NMR. ‡ Obtained from GPC.

Table S2.

Properties of the gyroidal mesoporous carbon (G^DMC).

Name	ISO:resols (weight ratio)	Mesopore surface area*	Pore volume†	Porosity‡	Unit cell size§
G^DMC	1 : 0.54	94 m^2/g	0.86 cm^3/g	63 vol%	129 nm

* Calculated from the difference of the BET surface area and the t-plot micropore surface area. † Derived from the total adsorbed nitrogen volume at a relative pressure of 0.99. ‡ Calculated using the pore volume and the specific volume of 0.5 cm^3/g for carbon. § Derived from small angle X-ray scattering (SAXS).

Detailed experimental procedures.

Gyroidal mesoporous carbon (G^DMC). The G^DMC monoliths were synthesized using block copolymer (BCP) self-assembly. The structure directing amphiphilic triblock terpolymer poly(isoprene)-*block*-poly(styrene)-*block*-poly(ethylene oxide) (PI-*b*-PS-*b*-PEO, ISO) was synthesized via a step-wise anionic polymerization[1]. The characteristics of the ISO are summarized in Supplementary table 1. Phenol-formaldehyde resols were used as carbon precursors and synthesized using oligomerization of phenol and formaldehyde in a molar ratio of 1:2 under basic conditions[2]. Monolithic ISO:resols hybrids with double gyroidal (G^D) morphology were obtained by dissolution of both components in a 1:0.54 weight ratio in tetrahydrofuran (THF) and chloroform (1:1 by weight) and solvent evaporation at 50 °C in a Teflon dish. The dry films were annealed at 125 °C for 24 hours prior to carbonization. Irrespective of morphology, it is common in block copolymer (BCP) self-assembly to observe lamellar layers on surfaces of cast films due to surface energy differences between individual blocks and their corresponding affinity to air and the casting dish material[2]. These surface reconstituted lamellar capping layers were removed using an argon-oxygen plasma treatment for 40 mins on the polymeric-organic hybrid films, prior to carbonization. This treatment is essential to make the interior porosity accessible from the surfaces, after carbonization. Powdered G^DMC materials for characterization of the bulk properties, as well as G^DMC monoliths were carbonized at temperatures above 1000 °C under inert gas (argon/nitrogen) flow[2]. Characterization results and properties of the G^DMCs are shown in Fig. 1 and Supplementary Fig. 1, and summarized in Supplementary Table 2. The conductivity of the gyroidal mesoporous carbons ranged from 0.1 S cm^{-1} to 2 S cm^{-1} depending on the carbonization temperature[2]. Discussion of the detailed characterization of the conducting gyroidal mesoporous carbon materials can be found in Reference [2]. Free-standing G^DMC monoliths were cut into rectangular shapes with footprint areas of 0.08-0.14 cm^2, attached to a wire in an edge-on geometry with silver epoxy (EPO-TEK H20E from EMS), and cured at 80 °C for at least 10 hours. The exposed silver contact was then sealed to the outside using silicone rubber adhesive sealant (Momentive RTV 108) and cured at room temperature for at least 24 hours. Insulating gyroidal mesoporous polymer (G^DMP) materials were obtained from the same ISO-resols hybrids as the G^DMCs, but were submitted to heat treatment at only 450 °C under nitrogen for 3 hours. At 450 °C, the phenol-formaldehyde resols form an insulating, cross-linked polymeric resin, while the structure directing ISO triblock terpolymer decomposes resulting in gyroidal mesoporous polymer materials[3].

Electrodeposition of polymer electrolyte. The walls and surfaces of the conductive and redox-active G^DMC electrodes were conformally coated with poly(phenylene oxide) (PPO) using self-limiting electropolymerization. The polymerization solution in acetonitrile was 0.05 M in phenol and tetramethylammonium hydroxide pentahydrate, and 0.1 M in tetrabutylammonium perchlorate (TBAP). The solution was kept under an inert gas atmosphere (nitrogen) to prevent oxidation of the deprotonated phenol. Wire-connected G^DMC monoliths were immersed completely into the solution and left soaking for 15 mins. Electropolymerization was conducted in a three-electrode set up with a platinum counter electrode and a Ag/Ag^+ reference electrode (silver wire in acetonitrile with 0.05 M silver perchlorate and 0.1 M TBAP) using a Metrohm Autolab PGSTAT204 potentiostat. Cyclic voltammetry (CV) of phenol in basic solution on G^DMCs showed a broad irreversible oxidation peak around 0.08 V vs. Ag/Ag^+ that decayed rapidly with continuous cycling (Fig. 2a). No indication of an oxidation peak nor large double layer current was present after 10 cycles, indicating blockage of the surface pores and mesoporosity due to the electropolymerization reaction. To afford a thin and dense PPO film, phenol was oxidatively polymerized using pulsed potentiostatic deposition (Fig. 2b). 200 pulses at +0.6 V vs. Ag/Ag^+, well above the peak oxidation current in the mass transport limit, were employed for a duration of 5 sec with a 10 sec equilibration between each pulse, to allow for sufficient monomer diffusion into the mesopores[4]. In comparison to the electropolymerization, the background response of the electrolyte showed only double layer current with very little (if any) changes in the current response over 200 pulses (Supplementary Fig. 2a). Pulsed polymer electrodeposition was followed by cyclic voltammetric sweeps between -0.4 V and +0.6 V vs. Ag/Ag^+ at 20 mV s^{-1}. These cyclic voltammograms (CVs) after potentiostatic PPO deposition in the polymerization solution showed no oxidation peak occurring at the oxidation potential of the phenolate ion (compare Fig. 2a and Fig. 2c). The double layer response of the PPO coated G^DMCs showed a much larger CV-area than a flat substrate with the same geometrical surface area (Supplementary Figs. 2b,c), corroborating retained accessibility of mesopores after PPO electropolymerization. The mesoporous PPO-coated carbon monoliths were subsequently soaked in ethanol to remove excess electrolyte and dried at room temperature.

Lithiation-delithiation of G^DMC-electrolyte assembly. PPO-coated G^DMC monoliths and lithium foil were immersed in 1 M lithium perchlorate in dimethyl carbonate and ethylcarbonate (1:1 by volume) in a septum capped vial under an argon atmosphere. After soaking for 2 days, G^DMCs were galvanostatically lithiated/delithiated at 0.1 mA cm^{-2} to 0 V and 2 V vs. Li/Li^+, respectively, in a two-electrode setup using an MTI BT8 battery tester. The first discharge (lithiation of carbon) curves exhibited a plateau around 1 V vs. Li/Li^+ and a very large capacity, as is commonly observed for the first discharge of carbon anode materials due to build-up of a solid-electrolyte interface (SEI, Supplementary Fig. 3)[5]. The following charge (delithiation) and discharge (lithiation) showed a capacity of 1 and 1.3 mAh cm^{-2}, respectively, demonstrating reversible lithium intercalation through the PPO electrolyte layer. Assuming a carbon loading of 5 mg cm^{-2}, the areal capacity corresponds to a specific capacity of approximately 200 mAh g^{-1}.

Sulfur infiltration. Sulfur, employed as the cathode material, was introduced into the mesopores of PPO-coated G^DMCs through liquid/vapor infiltration at 155 °C for 24 hours. To that end, excess sulfur powder (1-3 mg) was put on and around the monoliths (with footprint areas of 0.08-0.14 cm^2, see above) in a sealed glass container, and heated to 155 °C for 24 hours.

Integrated polymeric current collector infiltration. Poly(ethylenedioxythiophene) (PEDOT) was chemically polymerized inside the PPO-coated and sulfur infiltrated G^DMC monolith mesopores using oxidative polymerization. A 0.7 M iron (III) para-toluenesulfonate solution in ethanol was freshly prepared and EDOT was added to make a 1 M EDOT solution[6]. The G^DMC-PPO-sulfur monoliths were immersed in the solution with the wire connection above the liquid-air interface and kept for 20 mins at 4 °C. The 3-D nanohybrid was subsequently removed from the solution, dried at room temperature for at least 4 hours, and further dried at 80 °C for at least 6 hours. The sulfur-PEDOT nanostructured composite phase was then contacted with silver epoxy (EPO-TEK H20E from EMS) on one of the monolith's surfaces. The cured electrical contact was again sealed to the outside with silicone rubber adhesive sealant (Momentive RTV 108) and cured for 2 days at room temperature. We assume that unpolymerized residual EDOT monomer is removed during the subsequent drying/lithiation steps, in which the gyroidal nano-3-D battery is immersed and soaked in a mixture of dioxolane (DOL) and dimethoxyethane (DME), or is oxidized to PEDOT during charging of the gyroidal 3-D nanohybrid battery.

Sulfur lithiation and galvanostatic testing. The contacted penta-continuous and tetrafunctional monolithic nanohybrid was immersed horizontally (i.e. parallel to the gas-liquid interface) in 1 M lithium perchlorate in a mixture of dioxolane (DOL) and dimethoxyethane (DME) (1:1 by volume) together with a lithium foil in a septum capped vial under argon atmosphere. The electrolyte was chosen to avoid unwanted side reactions with polysulfides that carbonate-based electrolytes undergo[7]. After soaking for 2 days, the sulfur-PEDOT phase was discharged to 1 V vs. Li/Li^+ at a current of 0.125 mA cm^{-2} (Fig. 4a,b). After lithiation of the sulfur-PEDOT nanocomposite the lithium foil was disconnected, and the penta-continuous and tetrafunctional nanohybrids were cycled to 3 V at 0.125 mA cm^{-2} with the nanostructured G^DMC and sulfur-PEDOT phases connected as anode and cathode, respectively. Subsequently, the electrolyte was removed and the tetrafunctional gyroidal nanohybrids were charged to 3.5 Volts and discharged at 0.125 mA cm^{-2} with varying cut-off voltages as described in the text.

Characterization. Scanning electron microscopy (SEM) of carbonized samples was carried out on a Zeiss LEO 1550 FE-SEM or a Tescan Mira SEM operating at an accelerating voltage of 10-20 kV. The SEM was equipped with a Bruker energy dispersive spectrometer (EDS) for elemental analysis. SAXS measurements were performed on monolithic parent hybrid and resulting carbon materials at the Cornell High Energy Synchrotron Source (CHESS). The sample to detector distance was 2.6 m and the X-ray wavelength, λ, was 1.20 Å. The scattering vector, q, in the experiments was defined as $q = (4\cdot\pi/\lambda)\cdot\sin\theta$, where θ is half of the scattering angle. Nitrogen sorption isotherms were obtained on a Micromeritics ASAP 2020 surface area and porosity analyzer at -196 °C. Lithiation and galvanostatic tests of monolithic carbon materials and tetrafunctional nanohybrids were executed using a BST8-WA 8-channel battery analyzer from MTI Corporation. Resistances through the PPO thin film of the PPO-coated G^DMC monoliths and of the PEDOT and sulfur-PEDOT infiltrated insulating gyroidal mesoporous polymer (G^DMP) frameworks were measured using cyclic voltammetry at a scan rate of 50 mV s^{-1} with an AUTOLAB Metrohm Autolab PGSTAT204. The second contact for the uncoated and PPO-coated carbon monoliths for resistance and electrochemical impedance spectroscopy measurements were made using a liquid gallium-indium eutectic contact on one of the surfaces. Contacts for the PEDOT and sulfur-PEDOT infiltrated insulating G^DMP framework were made with silver epoxy (EPO-TEK H20E from EMS) on both surfaces.

References

1 T. S. Bailey, C. M. Hardy, T. H. Epps and F. S. Bates, *Macromolecules*, 2002, **35**, 7007–7017.

2 J. G. Werner, T. N. Hoheisel and U. Wiesner, *ACS Nano*, 2014, **8**, 731–743.

3 Y. Meng, D. Gu, F. Zhang, Y. Shi, L. Cheng, D. Feng, Z. Wu, Z. Chen, Y. Wan, A. Stein and D. Zhao, *Chem. Mater.*, 2006, **18**, 4447–4464.

4 R. L. McCarley, E. a. Irene and R. W. Murray, *J. Phys. Chem.*, 1991, **95**, 2492–2498.

5 W. Xing, P. Bai, Z. F. Li, R. J. Yu, Z. F. Yan, G. Q. Lu and L. M. Lu, *Electrochim. Acta*, 2006, **51**, 4626–4633.

6 K. H. Hong, K. W. Oh and T. J. Kang, *J. Appl. Polym. Sci.*, 2005, **97**, 1326–1332.

7 J. Gao, M. A. Lowe, Y. Kiya and H. D. Abruña, *J. Phys. Chem. C*, 2011, **115**, 25132–25137.